Placental Malaria Induces a Unique Methylation Profile Associated with Fetal Growth Restriction

Nida Ozarslan[1,2], Corina Mong[1,2], John Ategeka[3], Lin Li[1,2], Sirirak Buarpung[1,2], Joshua F. Robinson[2], Jimmy Kizza[3], Abel Kakuru[3], Moses R. Kamya[3,4], Grant Dorsey[5], Philip J. Rosenthal[5], Stephanie L. Gaw[1,2]*

[1]Division of Maternal-Fetal Medicine, Department of Obstetrics, Gynecology & Reproductive Sciences, University of California, San Francisco (UCSF); San Francisco, CA, USA.

[2] Center for Reproductive Sciences and Department of Obstetrics, Gynecology, and Reproductive Sciences, University of California, San Francisco (UCSF); San Francisco, CA, USA.

[3] Infectious Diseases Research Collaboration; Uganda.

[4] Department of Medicine, Makerere University; Kampala, Uganda.

[5] Division of HIV, Global Medicine, and Infectious Diseases, Department of Medicine, University of California, San Francisco; San Francisco, CA, USA.

Keywords: pregnancy, placenta, malaria, epigenetics, methylation, fetal programming, fetal growth restriction, IUGR, *Plasmodium falciparum*

* Correspondence:

Stephanie L. Gaw, MD, PhD
Associate Professor
Division of Maternal-Fetal Medicine
Center for Reproductive Sciences
Department of Obstetrics, Gynecology and Reproductive Sciences
University of California, San Francisco
513 Parnassus Ave, Box 0556 16HSE

24 San Francisco, CA 94143

25 E-mail: Stephanie.Gaw@ucsf.edu

26 **Abstract**

27 Background: Fetal growth restriction (FGR) is associated with perinatal death and adverse birth
28 outcomes, as well as long-term complications, including increased childhood morbidity, abnormal
29 neurodevelopment, and cardio-metabolic diseases in adulthood. Placental epigenetic reprogramming
30 associated with FGR may mediate these long-term outcomes. Placental malaria (PM), characterized by
31 sequestration of *Plasmodium falciparum*-infected erythrocytes in placental intervillous space, is the
32 leading global cause of FGR, but its impact on placental epigenetics is unknown. We hypothesized that
33 placental methylomic profiling would reveal common and distinct mechanistic pathways of non-malarial
34 and PM-associated FGR.

35 Results: We analyzed placentas from a US cohort with no malaria exposure (n = 12) and a cohort from
36 eastern Uganda, a region with a high prevalence of malaria (n = 12). From each site, 8 cases of FGR
37 (defined as birth weight <10%ile for gestational age by Intergrowth-21 standard curves) and 4 healthy
38 controls with normal weight were analyzed. PM was diagnosed by placental histopathology. We
39 compared the methylation levels of over 850K CpGs of the placentas using Infinium MethylationEPIC v1
40 microarray. Non-malarial FGR was associated with 65 differentially methylated CpGs (DMCs), whereas
41 PM-FGR was associated with 133 DMCs, compared to their corresponding controls without FGR. One
42 DMC (cg16389901, located in the promoter region of *BMP4*) was commonly hypomethylated in both
43 groups. We identified 522 DMCs between non-malarial FGR vs. PM-FGR placentas, which was
44 independent of differing geographic location or cellular composition.

45 Conclusion: Placentas with PM-associated FGR have distinct methylation profiles as compared to
46 placentas with non-malarial FGR, suggesting novel epigenetic reprogramming in response to malaria.
47 Larger cohort studies are needed to determine the distinct long-term health outcomes in PM-associated
48 FGR pregnancies.

49

Background

Malaria in pregnancy leads to adverse birth outcomes including fetal growth restriction (FGR), low birth weight, preterm birth, and fetal loss. In 2022, 12.7 million pregnant individuals in sub-Saharan Africa were exposed to malaria, potentially resulting in an estimated 914,000 babies being born with low birth weight in the absence of pregnancy-specific chemoprevention Placental malaria (PM), characterized by the sequestration of *Plasmodium falciparum*-infected red blood cells (RBCs) in the placental intervillous spaces, has been independently associated with small for gestational age deliveries and poor neurodevelopmental outcomes (1–4). PM is the leading global cause of FGR. Two mechanisms have been proposed: 1) congestion and inflammation, secondary to the sequestration of infected RBCs in the intervillous spaces during pregnancy, disrupt trophoblast invasion and angiogenesis, decreasing umbilical artery flow (5–7); and 2) vascular dysfunction and chronic inflammation contribute to impaired nutrient exchange at the fetal-maternal interface and imbalances in growth factors (8).

Fetal growth is evaluated by in utero ultrasonographic measurements of fetal biometric measurements (9). FGR is defined as an estimated fetal weight or abdominal circumference less than the 10th percentile for gestational age (10). FGR has important influences on human health. Early onset FGR (<32 weeks gestation) and severe FGR (<3rd percentile) are associated with up to 1.5-fold increased risk of stillbirth and a 2 to 5-fold risk of perinatal death (11). Long-term complications of FGR include increased childhood morbidity and cardiovascular, metabolic, and neuropsychiatric diseases in adulthood (2,4,12–24). In areas with no malaria risk, the etiologies of FGR include maternal comorbidities such as hypertension, autoimmune disease, renal insufficiency as well as placental dysfunction, genetic abnormalities, and environmental exposures (10).

PM and FGR independently impact infant growth and neurodevelopment (25–29). These long-term health impacts may be mediated through epigenetic modifications, including DNA methylation, histone marks, and expression of non-coding RNAs (30–32). For example, placental epigenetic modifications proximal to genes such as IGF2, AHRR, HSD11B2, WNT2, and FOLS1 were found to be associated with FGR (33,34). In contrast, epigenetic studies of human responses to malaria have been largely focused on immune markers of disease susceptibility (35,36). Altered DNA methylation has been demonstrated in monocytes after malaria infection, resulting in age-dependent changes in innate immune

78 and inflammatory responses (37,38). To our knowledge, no studies have examined the epigenetic
79 interactions among FGR and PM-inflicted pregnancies, although existing evidence suggests the potential
80 for shared and divergent mechanisms contributing to altered fetal programming. In this study, we
81 compared methylation profiles in placentas of non-malarial and PM-associated pregnancies, with or
82 without FGR.

83 **Methods**

84 Study design and subjects

85 Placental samples were collected from two independent patient cohorts. Cohort 1 (no malaria) was
86 comprised of 12 placental samples prospectively collected at the University of California, San Francisco,
87 United States (US) from 2018 to 2022 (IRB #10-00505, #20-32077 and #21-33986). Cohort 2 (malaria
88 endemic) was comprised of 12 placental samples prospectively collected from 2021-2022 in Busia,
89 Uganda, as part of a randomized controlled trial of intermittent preventative treatment for malaria in
90 pregnancy (NCT04336189, IRB#19-29105).

91 Case definitions: All patients were primigravidas and had no evidence of fetal genetic or structural
92 anomalies. FGR cases were identified by estimated fetal weight < 10th percentile for gestational age on
93 all prenatal ultrasounds throughout pregnancy (up to 4 were performed) and birth weight <10th percentile
94 for gestational age by Intergrowth-21 birth weight standards (39). PM-FGR cases were complicated by
95 both FGR and placental malaria (PM) diagnosed by placental histopathology according to Rogerson
96 criteria (40). The presence of *Plasmodium* parasites indicated active PM, whereas malaria pigment
97 (hemozoin) accumulation in the placental tissue was classified as chronic PM (41). Control cases from
98 each cohort were from healthy pregnancies with no pregnancy complications and no evidence of malaria
99 in pregnancy at any time during the study (for Cohort 2). Samples were divided into four groups: 1) FGR
100 (no malarial FGR, n=8), 2) C^{FGR} (healthy controls from the US, n=4), 3) PM-FGR (placental malaria
101 associated FGR, n=8), and 4) $C^{PM\text{-}FGR}$ (healthy controls from Uganda, n=4; **Figure 1A**). Detailed case
102 information is provided in **Supplemental Table 1.**

103 Specimen collection

104 Placental biopsies were collected from the maternal side of the placenta within 1 hour of delivery.
105 Biopsies no larger than 5 x 10 x 10mm were washed with ice-cold PBS three times and placed in
106 RNAlater™ (Qiagen, Germantown, MD). After a minimum incubation of 24 hours in RNAlater at 4°C,
107 biopsies were frozen and stored at -80°C. The same protocol was followed at both sites.

108 DNA extraction

109 DNA was extracted from placental biopsies using a DNeasy Blood & Tissue Kit (Qiagen, Germantown,
110 MD) according to the manufacturer's standard protocol. Samples were treated with RNase for 2 minutes.
111 Infinite M NanoQuant (Tecan, Morrisville, NC) was used to estimate the purity and concentration of
112 extracted DNA. The A260/A280 ratio for all samples was between 1.75-1.93.

113 Infinium MethylationEPIC v1 Assay

114 We profiled global methylation of DNA aliquots of placental samples. In brief, bisulfate conversion of 1μg
115 DNA/sample was performed using and the EZ DNA Methylation-Lightning Kit (Zymo Research, Irvine,
116 CA). Bisulfite converted DNA was amplified, fragmented, precipitated, resuspended, and hybridized to
117 Infinium Methylation EPIC v1.0 (Illumina, San Diego, CA) arrays following the manufacturer's protocol.
118 Arrays were washed to remove any unspecific binding, extended and stained primers and imaged using
119 iScan (Illumina, San Diego, CA) platform.

120 RNA extraction and qRT-PCR

121 RNA was extracted from placental biopsies using RNeasy Mini Kit (Qiagen, Germantown, MD) according
122 to the manufacturer's standard protocol. Infinite M NanoQuant (Tecan, Morrisville, NC) was used to
123 estimate the purity and concentration of extracted RNA. The A260/A280 ratio for all samples was
124 between 2.11-2.19. We converted 500 ng of purified RNA to cDNA using qScript cDNA synthesis kit
125 (Quantabio, Beverly, MA), and performed qRT-PCR using TaqMan primer for *BMP4* (Hs03676628_s1)
126 mixed with TaqMan Universal Master Mix II, no UNG (Life Technologies, Quant Studio 6). Reactions were
127 carried out for 40 cycles. At least 3 technical replicates were analyzed for all comparisons. The

128 expression level of *BMP4* was calculated via the ΔΔCT method. We normalized expression using the
129 mean CT of the housekeeping gene, GAPDH (Hs02786624_g1).

130 Bioinformatic analysis

131 The raw data obtained from the iScan platform was cleaned and preprocessed for data analysis using R
132 (version 4.2.1) and minfi package (version 1.44.0). The quality of the samples was assessed by
133 computing detection p-values for all probes. Low-quality probes that failed at a detection p-value of 0.05
134 in at least 10% of the samples, probes located on the sex chromosome (X and Y), probes with SNPs at
135 the CpG site, and cross-reactive probes were filtered out prior to quantile normalization and differential
136 methylation analysis. No samples were excluded based on high p-value probes. The total number of
137 probes before filtering was 865,859, whereas total number of probes after filtering was 786,227.

138 Differential methylation analysis was performed by first computing M values, i.e., the log ratios of
139 methylated vs. unmethylated signal intensities for each probe and limma (version 3.54.2) implemented in
140 the R-package minfi package. Secondly, β-values were calculated, representing the total % methylation
141 level of each CpG site. We performed 4 pairwise comparisons: 1) FGR vs. C^{FGR}; 2) PM-FGR vs. $C^{PM\text{-}FGR}$;
142 3) C^{FGR} vs. $C^{PM\text{-}FGR}$; 4) FGR vs. PM-FGR. In comparisons among groups, differentially methylated CpGs
143 (DMC) were identified based on an unadjusted *p*-value < 0.0001 and an absolute average difference in
144 methylation (|Δβ|) > 10% (test group vs. control group). Genes proximal to DMCs, were identified using
145 the University of California, Santa Cruz Genome Browser(42). Functional gene ontology (GO) enrichment
146 analysis of genes associated with DMCs was conducted using the Database for Annotation, Visualization
147 and Integrated Discovery (DAVID)(43). For qRT-PCR, we conducted Mann-Whitney test between
148 pairwise comparisons to determine significant differences in expression (p<0.05). Cellular deconvolution
149 analysis was conducted using *planet* (v1.12) package on R (44). Figures were generated using R Studio
150 (v2023.03.0+386), GraphPad Prism (v10.2.3) and BioRender.

151 **Results**

152 Characteristics of study participants

153 To search for associations between FGR types and methylation patterns in samples from the US and

154 Uganda we selected a total of 24 placentas divided into four groups: C^{FGR} (n=4), $C^{PM\text{-}FGR}$ (n=4). FGR
155 (n=8), and PM-FGR (n=8). The median and interquartile ranges for gestational age, birth weight and
156 Intergrowth-21 birth weight percentiles and the percentage of female infants were provided in **Table 1**.

Table 1. Study group characteristics.

Characteristics	**FGR (n=8)**	**C^{FGR} (n=4)**	**PM-FGR (n=8)**	**$C^{PM\text{-}FGR}$ (n=4)**
Gestational age	37.5 (36.7-38.2)	39.2 (39.1-39.5)	39.8 (39.1-41.2)	39.2 (38.3-40.1)
Birth weight (gr)	2193 (2004-2355)	3565 (3048-3768)	2600 (2510-2843)	2915 (2885-3470)
Intergrowth-21 birth weight percentile	2.9 (1.1-5.5)	80.1 (30.1-87.7)	3.9 (3.2-5.7)	29.4 (21.8-76.1)
Infant sex (female)	62.5%	25%	50%	75%

The median and interquartile ranges were provided for gestational age, birth weight and Intergrowth-21 birth weight percentiles. Percentage of female infants were provided for infant sex.

157 Dimensional Reduction Analysis

158 We profiled the methylome of our selected placentas using Illumina Infinium MethylationEPIC Arrays v1.
159 After applying quality control measures, we compared methylation patterns of 786,227 CpG sites among
160 FGR, PM-FGR, and respective controls, C^{FGR} and $C^{PM\text{-}FGR}$, from the two unique geographic locations.
161 Unsupervised principal component analysis using M-values of all CpG sites suggested no overall distinct
162 separation among the four groups, suggesting general similarities in global methylation profiles
163 independent of FGR or PM-FGR status or collection site (**Figure 1B-E**). In pairwise comparisons
164 between groups, separation was most prominent between FGR and PM-FGR groups (**Figure 1F**).

165 Identification of Differentially Methylated CpGs

166 To better characterize differences in methylation levels with non-malarial FGR and PM-associated FGR
167 we investigated the differentially methylated CpGs using an unadjusted p value cutoff of $p<0.0001$ and a
168 secondary cutoff of at least 10% absolute difference in mean methylation ($|\Delta\beta| > 0.10$). To confirm the
169 power of the significance cutoff in terms of differentiating the groups, unsupervised hierarchical clustering
170 was performed using β-values of the respective DMCs. As expected, our samples clustered based on
171 study group (**Supplemental Figure 1, Supplemental Data 1**).

172 Differentially Methylated CpGs with FGR

173 We first investigated the influence of non-malarial FGR on placental methylation profiles in comparison
174 with their respective geographic controls. We identified 65 DMCs, that were distributed across all
175 autosomal chromosomes except for chromosomes 19 and 21 (**Figure 2A**). Of the 65 DMCs, 48 were
176 hypomethylated and 17 were hypermethylated with non-malarial FGR vs. C^{FGR} (**Figure 2B**). While most of
177 the DMCs were located at the body and intergenic regions, 14 hypomethylated CpGs and 6
178 hypermethylated CpGs were located in the promoter or 1st exon region (**Figure 2C)**. Functional
179 enrichment analysis through DAVID revealed that the genes associated with the 14 hypomethylated
180 CpGs located in the promoter or 1st exon region were involved in transport, cellular response to stress,
181 nephron development and localization within membrane; in contrast, the 6 hypermethylated CpGs were
182 associated with genes involved in angiogenesis.

183

184 Differentially Methylated CpGs with PM-FGR

185 Next, we investigated the DMCs between PM-FGR vs. $C^{PM\text{-}FGR}$, we identified 133 CpGs that were
186 distributed across all autosomal chromosomes with the exception of chromosome 9 (**Figure 2D**). Of the
187 133 DMCs, 82 were hypomethylated and 51 were hypermethylated with non-malarial FGR vs. C^{FGR}
188 (**Figure 2E**). While most of the DMCs were located at the body and intergenic regions, 12
189 hypomethylated CpGs and 10 hypermethylated CpGs were located in the promoter or 1st exon region
190 (**Figure 2F)**. Genes associated with the 12 hypomethylated CpGs located in the promoter or 1st exon
191 region were involved in signaling; the 6 hypermethylated CpGs were associated with genes involved in
192 cell differentiation, tissue development and transport across the membrane.

193 Common changes observed with non-malarial FGR and PM-FGR

194 To identify the epigenetic modulations observed with both non-malarial and PM-FGR, we investigated the
195 overlapping DMCs between FGR vs. C^{FGR} and PM-FGR vs. $C^{PM\text{-}FGR}$ comparisons. We identified only a
196 single CpG, cg16389901, that was commonly hypomethylated with both FGR and PM-FGR when
197 compared to their respective controls (**Figure 3A**). In comparing trends in methylation patterns among
198 DMCs identified in either disease group, we observed distinct patterns between non-malarial FGR and
199 PM-FGR (**Figure 3B-3C**). The commonly hypomethylated CpG site cg16389901 is in the promoter region

200 of two splice variants of *BMP4*, a cell growth-related gene known to participate in trophoblast
201 differentiation within the placenta (45) (**Figure 3D**). Interestingly, DNA methylation levels of other CpGs
202 associated with *BMP4* did not show a difference between FGR vs. C^{FGR} or PM-FGR vs. $C^{PM\text{-}FGR}$
203 comparisons, suggesting a specific association with FGR. To understand the impact of differential DNA
204 methylation on the mRNA level we conducted qRT-PCR targeting *BMP4*. The mRNA expression levels of
205 *BMP4* did not show any significant difference between the four study groups (**Figure 3E**).

206 <u>Differentially methylated CpGs between FGR vs. PM-FGR</u>

207 We next compared the methylation profiles between FGR and PM-FGR. To account for baseline
208 epigenetic differences based on the distinct geographical locations of the two cohorts, we compared the
209 DMCs between the two control groups (C^{FGR} vs. $C^{PM\text{-}FGR}$), showing 183 CpGs that were differentially
210 methylated between the two study sites. Of these 183 DMCs, 7 CpG sites were also identified when
211 comparing FGR vs. PM-FGR. The exclusion of these 7 CpGs as potentially affected by population-based
212 differences resulted in 522 CpGs that were associated with PM status (**Figure 4A**). The number of DMCs
213 identified between FGR vs. PM-FGR was more than 8-fold than identified between FGR vs. C^{FGR} and 3-
214 fold between PM-FGR vs. $C^{PM\text{-}FGR}$ comparisons, highlighting the distinct changes observed with PM. The
215 522 DMCs were distributed across all autosomal chromosomes (**Figure 4B**). Of the 522 DMCs, 143 were
216 hypermethylated in non-malarial FGR placentas and 379 were hypermethylated in PM-FGR placentas
217 (**Figure 4C**). While most of the DMCs were located at the body and intergenic regions, 30
218 hypermethylated CpGs with FGR and 106 CpGs hypermethylated with PM-FGR were located in the
219 promoter or 1st exon region (**Figure 4D)**. Genes associated with the 30 hypermethylated CpGs with FGR
220 located in the promoter or 1st exon region were involved in actin cytoskeleton organization, whereas the
221 106 hypermethylated CpGs with PM-FGR were associated with genes involved in multicellular organism
222 development, regulation of metabolic processes, nervous system process, cell differentiation and
223 response to growth factor. Particularly, 3 CpG sites in the promoter region of *ARPC1B* and 4 CpG sites in
224 the promoter region of *ZSCAN23* were hypermethylated with FGR. On the other hand, 7 CpG sites in the
225 promoter region of *FAM124B* and 4 CpG sites in the promoter region of *SPG7* were hypermethylated with
226 PM-FGR.
227

228 Identifying the cellular composition of all placental samples

229 Our study used DNA extracted from homogenized placental tissue. To understand the cellular
230 composition of each sample, we performed cellular deconvolution analysis based on reference
231 methylation data of term placental cells generated by Yuan et al. (44) (**Figure 5A**). The robust partial
232 correlations (RPC) method was used to identify the percentages of syncytiotrophoblasts, trophoblasts,
233 endothelial cells, stromal cells, Hofbauer cells and nucleated red blood cells (nRBC) based on β-values of
234 the most distinguishing CpG sites among these cell types. As expected, our placental samples were
235 predicted based to be enriched for syncytiotrophoblasts, constituting an average of 69.5% of all cells. The
236 next most prevalent cell types were stromal cells (13.9%), endothelial cells (12.1%), and trophoblasts
237 (3.8%). The average abundance of Hofbauer cells and nRBC in total was less than 0.6%. We performed
238 unsupervised hierarchical clustering to investigate whether the cellular composition of samples differed
239 between the four study groups (**Figure 5B**). Overall, the cellular composition of samples did not show any
240 clear separation between groups (**Figure 5B, Supplemental Figure 2**). However, hierarchical clustering
241 of only FGR and PM-FGR samples demonstrated a more prominent clustering between the two groups
242 (**Figure 5C**). This separation was primarily associated with a significant increase in the percentage of
243 syncytiotrophoblasts in PM-FGR compared to FGR samples (74.4% vs. 65.5%, respectively; $p<0.002$).
244 Only a single CpG site overlapped with the 522 identified CpGs used for cellular deconvolution analysis,
245 indicating that DMCs identified between FGR vs. PM-FGR were unlikely to be driven by differences in
246 cellular composition (**Figure 5D**).

247 **Discussion**

248 To our knowledge, this is the first study to investigate methylation profiles in PM. We found that
249 placentas from non-malarial FGR and placental malaria-associated FGR cases exhibited highly divergent
250 methylation profiles. Interestingly, there was only a single CpG site, associated with the promoter region
251 of *BMP4,* that was commonly hypomethylated in placentas associated with both non-malarial FGR and
252 PM-FGR. In PM-FGR, hypermethylated CpGs were associated with genes encoding proteins involved in
253 developmental processes, whereas hypermethylated CpGs in FGR were associated with genes encoding
254 proteins involved in metabolic processes. Cellular deconvolution demonstrated differences in the relative

255 abundances of placental cell types between placentas associated with non-malarial and PM-FGR;
256 however, these differences did not explain the distinct methylation profiles of these groups. Overall, our
257 results suggest novel epigenetic modifications in response to PM-associated FGR compared to those
258 seen with non-malarial FGR.

259 Previous studies investigating placental epigenetic changes related to FGR in populations without
260 risk of malaria identified various differentially methylated CpG sites in genes encoding proteins involved
261 with fatty acid oxidation, transcriptional regulation, immune responses, cell adhesion, metabolism, and
262 cell growth (33,46–49). Similar to our study, one study from Korea investigating the methylation levels of
263 placenta and cord blood samples with FGR described changes in methylation profiles of genes encoding
264 proteins involved with metabolism and developmental pathways (48). While various studies investigated
265 methylation profiles of placenta, maternal blood or cord blood samples from pregnancies complicated with
266 fetal growth restriction, there was a lack of overlap of differentially methylated CpG sites as well as genes
267 related to those DMCs across these studies (33,34,46,47,49–52). Our results revealed unique
268 differentially methylated CpG sites and related genes compared to the previous FGR related studies.
269 Differences in results between studies may have been due to diverse mechanisms of epigenetic
270 modulation other than DNA methylation, such as histone modifications or non-coding RNA, as well as
271 differences in study populations.

272 In analyses of placentas, both non-malarial FGR and PM-FGR were associated with moderate
273 numbers of differentially methylated CpGs compared to their corresponding controls. Interestingly, a
274 single CpG site was commonly hypomethylated with both non-malarial FGR and PM-FGR—cg16389901.
275 This site is located 200-1500 bases upstream of the transcription start site of the *BMP4* gene. *BMP4* is a
276 well-studied growth-associated protein that also plays an important role in trophoblast differentiation
277 (45,53). The Korean study also described hypermethylation of genes encoding proteins involved in the
278 negative regulation of the BMP signaling pathway, which aligns with our results (48). Hypomethylation of
279 *BMP4*, resulting in increased expression, may be a common compensatory mechanism in the placenta to
280 counteract other functional changes that lead to inhibited fetal growth. In our placental samples, mRNA
281 levels of *BMP4* did not show any significant difference between our study groups. This could suggest that

282 the hypomethylation of *BMP4* with both non-malarial FGR and PM-FGR is a compensatory response to
283 normalize the mRNA levels in the setting of other mechanisms that may result in reduced expression of
284 this protein (e.g. histone modifications, posttranslational modifications)

285 Hypermethylated CpG sites in placentas from non-malarial FGR compared to PM-associated
286 FGR included CpGs located at the promoter regions of *ARPC1B* and *ZSCAN23*. Homozygous mutations
287 in the *ARPC1B* gene have been associated with disruptions in the immune system (54). Promoter region
288 hypermethylation of *ZSCAN23* has been associated with the acceleration of pancreatic cancer growth
289 (55). Conversely, hypermethylated CpG sites in placentas from PM-associated compared to non-malarial
290 FGR included CpGs located at the promoter regions of *FAM124B* and *SPG7*. *FAM124B* has been
291 proposed as an important protein involved in neurodevelopmental disorders, while SpG7 mutations have
292 been linked to spastic paraplegia and cerebellar ataxia (56,57). Further follow-up studies on offspring are
293 needed to investigate long-term outcomes associated with non-malarial FGR vs. PM-associated FGR and
294 to understand whether these outcomes are mediated by epigenetic mechanisms.

295 Cellular deconvolution analysis revealed dominance of syncytiotrophoblasts, which were present
296 in significantly higher proportions in PM-associated FGR samples. Differences in the proportion of
297 syncytiotrophoblasts may be associated with a classic pathological finding of syncytial knot formation
298 commonly observed with PM, which is thought to be a response to inflammatory damage associated with
299 infected RBCs in the intervillous spaces (58). Despite the differences in cellular composition, the
300 differentially methylated CpGs were distinct from those associated with specific cell types. In contrast, a
301 study that conducted the same deconvolution analysis on placentas from monochorionic twins with
302 selective FGR found decreased proportions of stromal cells in the twin with FGR compared to the
303 normally grown twin (46). This suggests that placental cellular composition may change in different
304 etiologies of FGR and warrants further study.

305 Our study has some limitations. First, we had a small sample size, and larger studies are needed
306 to confirm our findings. Second, due to the homogenization of placental tissue, we were unable to
307 distinguish between the origins of different cell types, particularly maternal and fetal immune cells. Third,

308 due to the high prevalence of malaria in pregnancy at our study site in Uganda, we did not identify any
309 FGR cases from Uganda without evidence of malaria infection during pregnancy; these cases would
310 provide a more direct comparison between non-malarial and PM-associated FGR in an African
311 population. Finally, we focused on methylation profiles detected by a targeted methylation array, rather
312 than whole genome bisulfide sequencing, which may identify additional differentially methylated CpGs.
313 Further studies investigating other types of epigenetic mechanisms such as histone modifications or
314 assessment of open chromatin regions would provide deeper insight into epigenetic changes occurring
315 with non-malarial and PM-associated FGR. Additional transcriptomic and proteomic analysis of similar
316 cohorts would also reveal insight into downstream effects of epigenetic modifications.

317 This is the first study, to our knowledge, comparing the methylation profiles of malarial and non-
318 malarial FGR in the placenta. Other strengths of our study include detailed characterizations of the
319 pregnancies, allowing for the selection of appropriate controls for each population. We only included
320 primigravid patients to avoid confounding from gravidity-induced differences in methylation profiles.
321 Finally, placental biopsies from both sites were collected and processed with the same protocol, allowing
322 for comparison between the different patient populations.

323 The significant differences that we found in DMCs in non-malarial and PM-associated FGR, even
324 after controlling for geographic location, suggest distinct pathways of epigenetic reprogramming in the
325 setting of FGR with or without PM. The independent and combined impact of placental malaria and
326 placental epigenetics may have potential implications for long-term health in the offspring.

327 **Declarations**

328 Ethics approval and consent to participate

329 This study was approved by the University of California, San Francisco and Makerere University. Written
330 informed consent was obtained from all participants.

331 Availability of data and materials

332 The dataset generated during the study will be available in the GEO repository (waiting for accession
333 number).

334 Competing interests

335 The authors declare that they have no competing interests.

336 Funding

337 This study was supported by the National Institutes of Health (NIAID K08AI141728 to SLG and

338 U01AI141308 to GD and PJR), and the Bill and Melinda Gates Foundation (INV-017035 to SLG).

339 Authors' contributions

340 Conceptualization: NO and SLG

341 Methodology: NO and SLG

342 Investigation: NO, CM, JA, LL, SB, JFR

343 Funding acquisition: MRK, GD, PJR, SLG

344 Project administration: AK, JK

345 Supervision: AK, SLG

346 Writing – original draft: NO and SLG

347 Writing – review & editing: All Authors

348 Acknowledgments

349 The authors thank all study participants. We also thank Keith Boohrer, Xiaojing Yang and Kai Chang from

350 the Zymo Research Corporation for their technical support.

351 **Figure Legends**

352 **Figure 1. Principal Component Analysis. A.** Schematic demonstration of study groups and collection

353 sites. **B.** Principal component analysis including all samples. **C.** Principal component analysis of FGR and

354 C^{FGR} samples. **D.** Principal component analysis of PM-FGR and $C^{PM\text{-}FGR}$ samples **E.** Principal component

355 analysis of C^{FGR} and $C^{PM\text{-}FGR}$ samples **F**. Principal component analysis of FGR and PM-FGR samples.

356 **Figure 2. Differentially methylated CpGs (DMCs) observed with non-malarial FGR and placental**

357 **malaria-associated FGR and their respective controls**. **A.** Manhattan plot of 65 DMCs ($p<0.0001$ and

358 $|\Delta\beta| > 0.1$) between FGR vs. C^{FGR} demonstrated by pink circles. **B.** Volcano plot displaying 48

359 hypomethylated and 17 were hypermethylated CpGs with FGR vs. C^{FGR} indicated by pink circles. **C.** Bar
360 graph demonstrating the distribution of hypermethylated (dark pink) and hypomethylated (light pink)
361 DMCs with FGR vs. C^{FGR} among CpG positions. **D.** Manhattan plot of 133 DMCs ($p<0.0001$ and $|\Delta\beta| >$
362 0.1) between PM-FGR vs. $C^{PM\text{-}FGR}$ demonstrated by teal circles. **E.** Volcano plot displaying 82
363 hypomethylated and 51 were hypermethylated CpGs with PM- FGR vs. $C^{PM\text{-}FGR}$ indicated by teal circles.
364 **F.** Bar graph demonstrating the distribution of hypermethylated (dark teal) and hypomethylated (light teal)
365 DMCs with PM- FGR vs. $C^{PM\text{-}FGR}$ among CpG positions.

366 **Figure 3. Commonly differentially methylated CpG site with non-malarial FGR and placental**
367 **malaria-associated FGR**. **A.** Venn diagram demonstrating the sole overlapping differentially methylated
368 CpG site, cg16389901, that was commonly hypomethylated with both non-malarial and placental malaria-
369 associated FGR when compared to their controls. **B.** Normalized methylation levels of all samples based
370 on their geographically matched control group average of 65 DMCs identified between FGR vs. C^{FGR} **C.**
371 Normalized methylation levels of all samples based on their geographically matched control group
372 average of 133 DMCs identified between PM-FGR vs. $C^{PM\text{-}FGR}$ **D.** Average DNA methylation of CpG sites
373 associated with *BMP4*, including cg16389901 (marked in red), for all four groups. Red asterisk indicates
374 significance. **E.** Gene expression levels of *BMP4* measured by qRT-PCR.

375 **Figure 4. Differentially methylated CpGs (DMCs) observed between non-malarial FGR vs. placental**
376 **malaria-associated FGR. A.** Venn diagram demonstrating the 522 DMCs ($p<0.0001$ and $|\Delta\beta| > 0.1$)
377 between FGR vs. PM-FGR after subtracting geographical location-driven baseline differences **B.**
378 Manhattan plot of 522 DMCs between FGR vs. PM-FGR demonstrated by purple circles. **C.** Volcano plot
379 displaying 143 hypermethylated CpGs in FGR and 379 CpGs hypermethylated in PM-FGR indicated by
380 purple circles. **D.** Bar graph demonstrating the distribution of hypermethylated CpGs with FGR (light
381 purple) and hypermethylated with PM-FGR (dark purple) among CpG positions.

382 **Figure 5. Cellular deconvolution analysis based on overall methylation levels. A.** Cell composition
383 of all samples estimated using robust partial correlations analysis through planet package in R. **B.**
384 Hierarchical clustering of all samples based on cellular deconvolution results. **C.** Hierarchical clustering of

385 FGR and PM-FGR samples based on cellular deconvolution analysis. **D.** Venn diagram demonstrating
386 the overlap between CpGs used for cellular deconvolution analysis and differentially methylated CpGs
387 between FGR vs. PM-FGR.

388 **Supplementary Documents**

389 **Supplementary Table 1. Patient characteristics.** cHTN; chronic hypertension, gHTN; gestational
390 hypertension, gDM; gestational DM, PreE; preeclampsia, SIPE; superimposed preeclampsia.

391 **Supplementary Figure 1. Hierarchical clustering of samples based on methylation levels of**
392 **differentially methylated CpGs (DMCs**). A. Methylation level of 65 DMCs between FGR vs. C^{FGR} **B.**
393 Methylation level of 133 DMCs between PM-FGR vs. $C^{PM\text{-}FGR}$ **C.** Methylation level of 183 DMCs between
394 C^{FGR} vs. $C^{PM\text{-}FGR}$ **D.** Methylation level of 522 DMCs between FGR vs. PM-FGR

395 **Supplementary Figure 2. Hierarchical clustering of samples based on cellular composition. A.**
396 Hierarchical clustering of FGR and C^{FGR} samples based on cellular composition**.** **B.** Hierarchical
397 clustering of PM-FGR and $C^{PM\text{-}FGR}$ samples based on cellular composition.

398 **Supplementary Data 1. List of differentially methylated CpG sites.**

399 **References**

400 1. Garrison A, Boivin MJ, Fiévet N, Zoumenou R, Alao JM, Massougbodji A, et al. The Effects of Malaria
401 in Pregnancy on Neurocognitive Development in Children at 1 and 6 Years of Age in Benin: A
402 Prospective Mother-Child Cohort. Clin Infect Dis Off Publ Infect Dis Soc Am. 2022 Mar 9;74(5):766–
403 75.

404 2. Bangirana P, Conroy AL, Opoka RO, Semrud-Clikeman M, Jang JH, Apayi C, et al. Effect of Malaria
405 and Malaria Chemoprevention Regimens in Pregnancy and Childhood on Neurodevelopmental and
406 Behavioral Outcomes in Children at 12, 24, and 36 Months: A Randomized Clinical Trial. Clin Infect
407 Dis. 2023 Feb 18;76(4):600–8.

408 3. Conroy AL, Bangirana P, Muhindo MK, Kakuru A, Jagannathan P, Opoka RO, et al. Case Report:
409 Birth Outcome and Neurodevelopment in Placental Malaria Discordant Twins. Am J Trop Med Hyg.
410 2019 Mar;100(3):552–5.

411 4. Bangirana P, Opoka RO, Boivin MJ, Idro R, Hodges JS, Romero RA, et al. Severe Malarial Anemia is
412 Associated With Long-term Neurocognitive Impairment. Clin Infect Dis. 2014 Aug 1;59(3):336–44.

413 5. Moore KA, Simpson JA, Wiladphaingern J, Min AM, Pimanpanarak M, Paw MK, et al. Influence of the
414 number and timing of malaria episodes during pregnancy on prematurity and small-for-gestational-
415 age in an area of low transmission. BMC Med. 2017 Dec;15(1):117.

416 6. Chua CLL, Khoo SKM, Ong JLE, Ramireddi GK, Yeo TW, Teo A. Malaria in Pregnancy: From
417 Placental Infection to Its Abnormal Development and Damage. Front Microbiol. 2021 Nov
418 11;12:777343.

419 7. Dorman EK, Shulman CE, Kingdom J, Bulmer JN, Mwendwa J, Peshu N, et al. Impaired
420 uteroplacental blood flow in pregnancies complicated by falciparum malaria: Uterine artery Doppler
421 and malaria. Ultrasound Obstet Gynecol. 2002 Feb;19(2):165–70.

422 8. Chandrasiri UP, Chua CLL, Umbers AJ, Chaluluka E, Glazier JD, Rogerson SJ, et al. Insight Into the
423 Pathogenesis of Fetal Growth Restriction in Placental Malaria: Decreased Placental Glucose
424 Transporter Isoform 1 Expression. J Infect Dis. 2014 May 15;209(10):1663–7.

425 9. Hadlock FP, Harrist RB, Martinez-Poyer J. In utero analysis of fetal growth: a sonographic weight
426 standard. Radiology. 1991 Oct;181(1):129–33.

427 10. ACOG Practice Bulletin No. 204: Fetal Growth Restriction. Obstet Gynecol. 2019 Feb;133(2):e97–
428 109.

429 11. Madden JV, Flatley CJ, Kumar S. Term small-for-gestational-age infants from low-risk women are at
430 significantly greater risk of adverse neonatal outcomes. Am J Obstet Gynecol. 2018
431 May;218(5):525.e1-525.e9.

432 12. Weckman AM, Conroy AL, Madanitsa M, Gnaneswaran B, McDonald CR, Kalilani-Phiri L, et al.
433 Neurocognitive outcomes in Malawian children exposed to malaria during pregnancy: An
434 observational birth cohort study. PLoS Med. 2021 Sep;18(9):e1003701.

435 13. Colella M, Frérot A, Novais ARB, Baud O. Neonatal and Long-Term Consequences of Fetal Growth
436 Restriction. Curr Pediatr Rev. 2018 Dec 21;14(4):212–8.

437 14. Lesseur C, Paquette AG, Marsit CJ. Epigenetic Regulation of Infant Neurobehavioral Outcomes. Med
438 Epigenetics. 2014 Jun 11;2(2):71–9.

439 15. Mericq V, Martinez-Aguayo A, Uauy R, Iñiguez G, Van Der Steen M, Hokken-Koelega A. Long-term
440 metabolic risk among children born premature or small for gestational age. Nat Rev Endocrinol. 2017
441 Jan;13(1):50–62.

442 16. D'Agostin M, Di Sipio Morgia C, Vento G, Nobile S. Long-term implications of fetal growth restriction.
443 World J Clin Cases. 2023 May 6;11(13):2855–63.

444 17. Chan PYL, Morris JM, Leslie GI, Kelly PJ, Gallery EDM. The Long-Term Effects of Prematurity and
445 Intrauterine Growth Restriction on Cardiovascular, Renal, and Metabolic Function. Int J Pediatr.
446 2010;2010:1–10.

447 18. Leon DA, Lithell HO, Vagero D, Koupilova I, Mohsen R, Berglund L, et al. Reduced fetal growth rate
448 and increased risk of death from ischaemic heart disease: cohort study of 15 000 Swedish men and
449 women born 1915-29. BMJ. 1998 Jul 25;317(7153):241–5.

450 19. Martyn CN, Barker DJ, Jespersen S, Greenwald S, Osmond C, Berry C. Growth in utero, adult blood
451 pressure, and arterial compliance. Heart. 1995 Feb 1;73(2):116–21.

452 20. Liefke J, Heijl C, Steding-Ehrenborg K, Morsing E, Arheden H, Ley D, et al. Fetal growth restriction
453 followed by very preterm birth is associated with smaller kidneys but preserved kidney function in
454 adolescence. Pediatr Nephrol Berl Ger. 2023 Jun;38(6):1855–66.

455 21. Senra JC, Yoshizaki CT, Doro GF, Ruano R, Gibelli MABC, Rodrigues AS, et al. Kidney impairment in
456 fetal growth restriction: three-dimensional evaluation of volume and vascularization. Prenat Diagn.
457 2020 Oct;40(11):1408–17.

458 22. Arigliani M, Stocco C, Valentini E, De Pieri C, Castriotta L, Ferrari ME, et al. Lung function between 8
459 and 15 years of age in very preterm infants with fetal growth restriction. Pediatr Res. 2021
460 Sep;90(3):657–63.

461 23. Nikolajev K, Heinonen K, Hakulinen A, Länsimies E. Effects of intrauterine growth retardation and
462 prematurity on spirometric flow values and lung volumes at school age in twin pairs. Pediatr
463 Pulmonol. 1998 Jun;25(6):367–70.

464 24. Grunnet LG, Bygbjerg IC, Mutabingwa TK, Lajeunesse-Trempe F, Nielsen J, Schmiegelow C, et al.
465 Influence of placental and peripheral malaria exposure in fetal life on cardiometabolic traits in adult
466 offspring. BMJ Open Diabetes Res Care. 2022 Apr;10(2):e002639.

467 25. Korzeniewski SJ, Allred EN, Joseph RM, Heeren T, Kuban KCK, O'Shea TM, et al.
468 Neurodevelopment at Age 10 Years of Children Born <28 Weeks With Fetal Growth Restriction.
469 Pediatrics. 2017 Nov 1;140(5):e20170697.

470 26. Leitner Y, Fattal-Valevski A, Geva R, Eshel R, Toledano-Alhadef H, Rotstein M, et al.
471 Neurodevelopmental outcome of children with intrauterine growth retardation: a longitudinal, 10-year
472 prospective study. J Child Neurol. 2007 May;22(5):580–7.

473 27. Murray E, Fernandes M, Fazel M, Kennedy S, Villar J, Stein A. Differential effect of intrauterine
474 growth restriction on childhood neurodevelopment: a systematic review. BJOG Int J Obstet Gynaecol.
475 2015 Jul;122(8):1062–72.

476 28. Elgueta D, Murgas P, Riquelme E, Yang G, Cancino GI. Consequences of Viral Infection and
477 Cytokine Production During Pregnancy on Brain Development in Offspring. Front Immunol. 2022 Apr
478 7;13:816619.

479 29. Sacchi C, Marino C, Nosarti C, Vieno A, Visentin S, Simonelli A. Association of Intrauterine Growth
480 Restriction and Small for Gestational Age Status With Childhood Cognitive Outcomes: A Systematic
481 Review and Meta-analysis. JAMA Pediatr. 2020 Aug 1;174(8):772.

482 30. Lapehn S, Paquette AG. The Placental Epigenome as a Molecular Link Between Prenatal Exposures
483 and Fetal Health Outcomes Through the DOHaD Hypothesis. Curr Environ Health Rep. 2022 Apr
484 29;9(3):490–501.

485 31. Nawathe AR, Christian M, Kim SH, Johnson M, Savvidou MD, Terzidou V. Insulin-like growth factor
486 axis in pregnancies affected by fetal growth disorders. Clin Epigenetics. 2016 Dec;8(1):11.

487 32. Lee MH, Jeon YJ, Lee SM, Park MH, Jung SC, Kim YJ. Placental gene expression is related to
488 glucose metabolism and fetal cord blood levels of insulin and insulin-like growth factors in intrauterine
489 growth restriction. Early Hum Dev. 2010 Jan;86(1):45–50.

490 33. Xiao X, Zhao Y, Jin R, Chen J, Wang X, Baccarelli A, et al. Fetal growth restriction and methylation of
491 growth-related genes in the placenta. Epigenomics. 2016 Jan;8(1):33–42.

492 34. Tekola-Ayele F, Zeng X, Ouidir M, Workalemahu T, Zhang C, Delahaye F, et al. DNA methylation loci
493 in placenta associated with birthweight and expression of genes relevant for early development and
494 adult diseases. Clin Epigenetics. 2020 Dec;12(1):78.

495 35. Arama C, Quin JE, Kouriba B, Östlund Farrants AK, Troye-Blomberg M, Doumbo OK. Epigenetics
496 and Malaria Susceptibility/Protection: A Missing Piece of the Puzzle. Front Immunol. 2018 Aug
497 3;9:1733.

498 36. Goldberg AD, Allis CD, Bernstein E. Epigenetics: A Landscape Takes Shape. Cell. 2007
499 Feb;128(4):635–8.

500 37. Dobbs KR, Embury P, Koech E, Ogolla S, Munga S, Kazura JW, et al. Age-related differences in
501 monocyte DNA methylation and immune function in healthy Kenyan adults and children. Immun
502 Ageing. 2021 Dec;18(1):11.

503 38. Romero DVL, Balendran T, Hasang W, Rogerson SJ, Aitken EH, Achuthan AA. Epigenetic and
504 transcriptional regulation of cytokine production by Plasmodium falciparum-exposed monocytes. Sci
505 Rep. 2024 Feb 5;14(1):2949.

506 39. Papageorghiou AT, Ohuma EO, Altman DG, Todros T, Ismail LC, Lambert A, et al. International
507 standards for fetal growth based on serial ultrasound measurements: the Fetal Growth Longitudinal
508 Study of the INTERGROWTH-21st Project. The Lancet. 2014 Sep;384(9946):869–79.

509 40. Rogerson SJ, Hviid L, Duffy PE, Leke RF, Taylor DW. Malaria in pregnancy: pathogenesis and
510 immunity. Lancet Infect Dis. 2007 Feb;7(2):105–17.

511 41. Zakama AK, Ozarslan N, Gaw SL. Placental Malaria. Curr Trop Med Rep. 2020 Dec;7(4):162–71.

512 42. Nassar LR, Barber GP, Benet-Pagès A, Casper J, Clawson H, Diekhans M, et al. The UCSC Genome
513 Browser database: 2023 update. Nucleic Acids Res. 2023 Jan 6;51(D1):D1188–95.

514 43. Sherman BT, Hao M, Qiu J, Jiao X, Baseler MW, Lane HC, et al. DAVID: a web server for functional
515 enrichment analysis and functional annotation of gene lists (2021 update). Nucleic Acids Res. 2022
516 Jul 5;50(W1):W216–21.

517 44. Yuan V, Hui D, Yin Y, Peñaherrera MS, Beristain AG, Robinson WP. Cell-specific characterization of
518 the placental methylome. BMC Genomics. 2021 Dec;22(1):6.

519 45. Xu RH, Chen X, Li DS, Li R, Addicks GC, Glennon C, et al. BMP4 initiates human embryonic stem
520 cell differentiation to trophoblast. Nat Biotechnol. 2002 Dec;20(12):1261–4.

521 46. Shi D, Zhou X, Cai L, Wei X, Zhang L, Sun Q, et al. Placental DNA methylation analysis of selective
522 fetal growth restriction in monochorionic twins reveals aberrant methylated *CYP11A1* gene for fetal
523 growth restriction. FASEB J. 2023 Oct;37(10):e23207.

524 47. Norton C, Clarke D, Holmstrom J, Stirland I, Reynolds PR, Jenkins TG, et al. Altered Epigenetic
525 Profiles in the Placenta of Preeclamptic and Intrauterine Growth Restriction Patients. Cells. 2023 Apr
526 11;12(8):1130.

527 48. Lee S, Kim YN, Im D, Cho SH, Kim J, Kim JH, et al. DNA Methylation and gene expression patterns
528 are widely altered in fetal growth restriction and associated with FGR development. Anim Cells Syst.
529 2021 May 4;25(3):128–35.

530 49. Monteagudo-Sánchez A, Sánchez-Delgado M, Mora JRH, Santamaría NT, Gratacós E, Esteller M, et
531 al. Differences in expression rather than methylation at placenta-specific imprinted loci is associated
532 with intrauterine growth restriction. Clin Epigenetics. 2019 Dec;11(1):35.

533 50. Roifman M, Choufani S, Turinsky AL, Drewlo S, Keating S, Brudno M, et al. Genome-wide placental
534 DNA methylation analysis of severely growth-discordant monochorionic twins reveals novel
535 epigenetic targets for intrauterine growth restriction. Clin Epigenetics. 2016 Dec;8(1):70.

536 51. Kantake M, Ikeda N, Nakaoka H, Ohkawa N, Tanaka T, Miyabayashi K, et al. IGF1 gene is
537 epigenetically activated in preterm infants with intrauterine growth restriction. Clin Epigenetics. 2020
538 Dec;12(1):108.

539 52. Richter AE, Bekkering-Bauer I, Verkaik-Schakel RN, Leeuwerke M, Tanis JC, Bilardo CM, et al.
540 Altered neurodevelopmental DNA methylation status after fetal growth restriction with brain-sparing. J
541 Dev Orig Health Dis. 2022 Jun;13(3):378–89.

542 53. Roberts RM, Ezashi T, Temple J, Owen JR, Soncin F, Parast MM. The role of BMP4 signaling in
543 trophoblast emergence from pluripotency. Cell Mol Life Sci. 2022 Aug;79(8):447.

544 54. Papadatou I, Marinakis N, Botsa E, Tzanoudaki M, Kanariou M, Orfanou I, et al. Case Report: A
545 Novel Synonymous ARPC1B Gene Mutation Causes a Syndrome of Combined Immunodeficiency,
546 Asthma, and Allergy With Significant Intrafamilial Clinical Heterogeneity. Front Immunol. 2021 Feb
547 19;12:634313.

548 55. Du Q, Zhang M, Gao A, He T, Guo M. Epigenetic silencing *ZSCAN23* promotes pancreatic cancer
549 growth by activating Wnt signaling. Cancer Biol Ther. 2024 Dec 31;25(1):2302924.

550 56. Batsukh T, Schulz Y, Wolf S, Rabe TI, Oellerich T, Urlaub H, et al. Identification and Characterization
551 of FAM124B as a Novel Component of a CHD7 and CHD8 Containing Complex. Englert C, editor.
552 PLoS ONE. 2012 Dec 21;7(12):e52640.

553 57. Care4Rare Canada Consortium, Choquet K, Tétreault M, Yang S, La Piana R, Dicaire MJ, et al.
554 SPG7 mutations explain a significant proportion of French Canadian spastic ataxia cases. Eur J Hum
555 Genet. 2016 Jul;24(7):1016–21.

556 58. Ismail MR, Ordi J, Menendez C, Ventura PJ, Aponte JJ, Kahigwa E, et al. Placental pathology in
557 malaria: A histological, immunohistochemical, and quantitative study. Hum Pathol. 2000
558 Jan;31(1):85–93.

559

Figure 1.

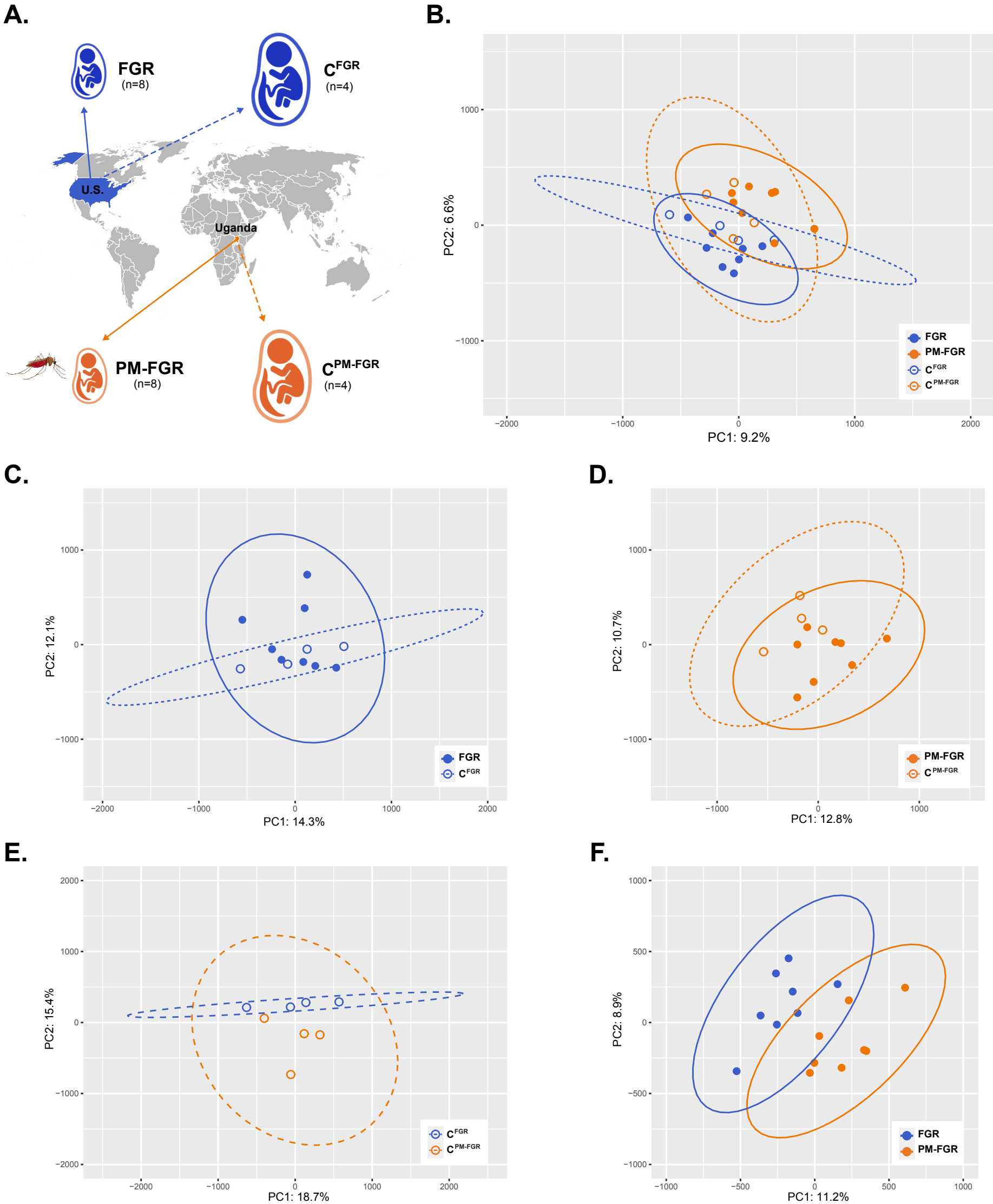
A.
FGR
(n=8)
C^FGR
(n=4)
U.S.
Uganda
PM-FGR
(n=8)
C^PM-FGR
(n=4)
B.
PC2: 6.6%
PC1: 9.2%
FGR
PM-FGR
C^FGR
C^PM-FGR
C.
PC2: 12.1%
PC1: 14.3%
FGR
C^FGR
D.
PC2: 10.7%
PC1: 12.8%
PM-FGR
C^PM-FGR
E.
PC2: 15.4%
PC1: 18.7%
C^FGR
C^PM-FGR
F.
PC2: 8.9%
PC1: 11.2%
FGR
PM-FGR

Figure 2.

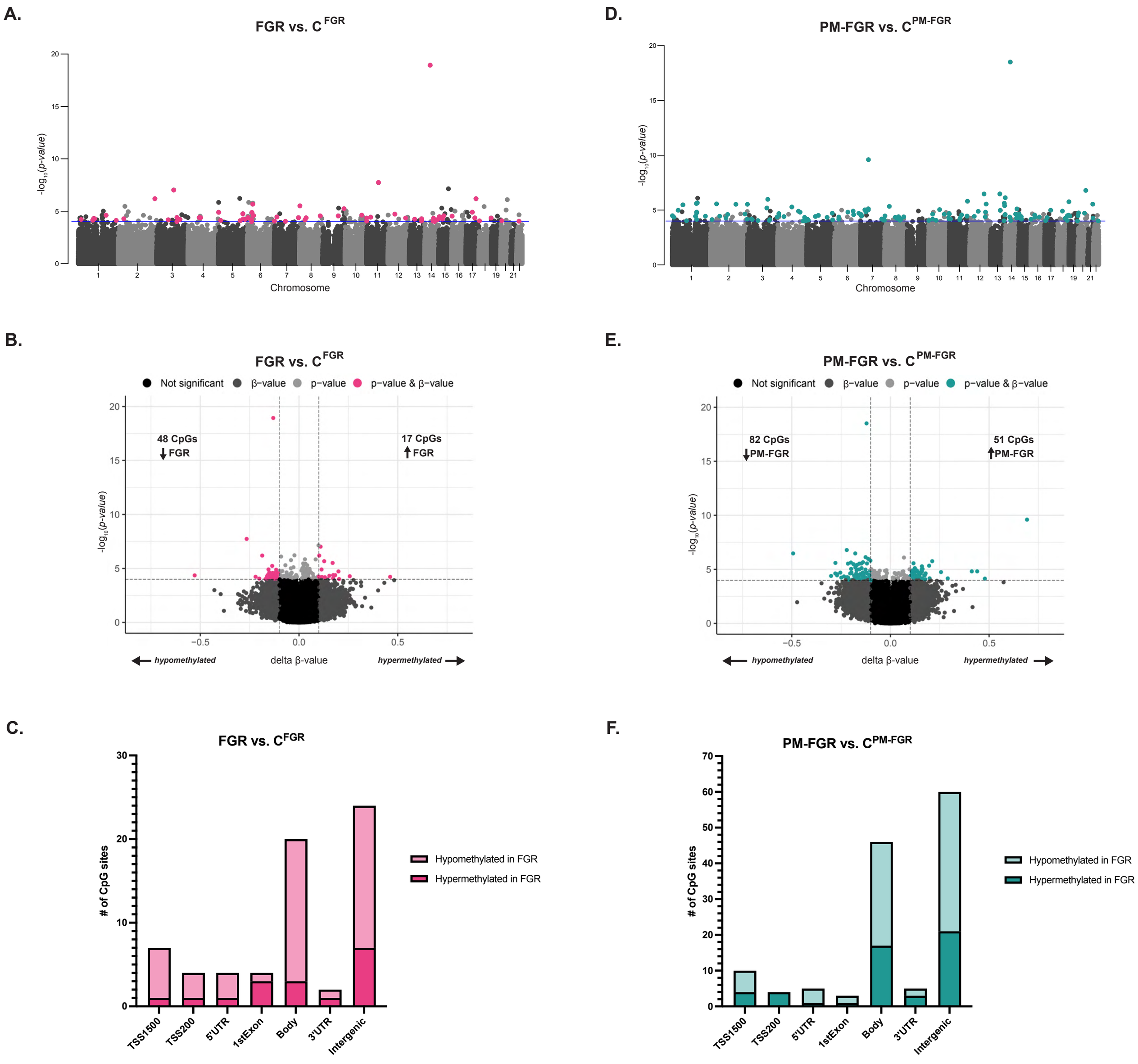
A.
FGR vs. C FGR
-log10(p-value)
Chromosome
D.
PM-FGR vs. C PM-FGR
-log10(p-value)
Chromosome
B.
FGR vs. C FGR
Not significant
β-value
p-value
p-value & β-value
48 CpGs
FGR
17 CpGs
FGR
-log10(p-value)
hypomethylated
delta β-value
hypermethylated
E.
PM-FGR vs. C PM-FGR
Not significant
β-value
p-value
p-value & β-value
82 CpGs
PM-FGR
51 CpGs
PM-FGR
-log10(p-value)
hypomethylated
delta β-value
hypermethylated
C.
FGR vs. CFGR
# of CpG sites
Hypomethylated in FGR
Hypermethylated in FGR
TSS1500
TSS200
5'UTR
1stExon
Body
3'UTR
Intergenic
F.
PM-FGR vs. CPM-FGR
# of CpG sites
Hypomethylated in FGR
Hypermethylated in FGR
TSS1500
TSS200
5'UTR
1stExon
Body
3'UTR
Intergenic

Figure 3.

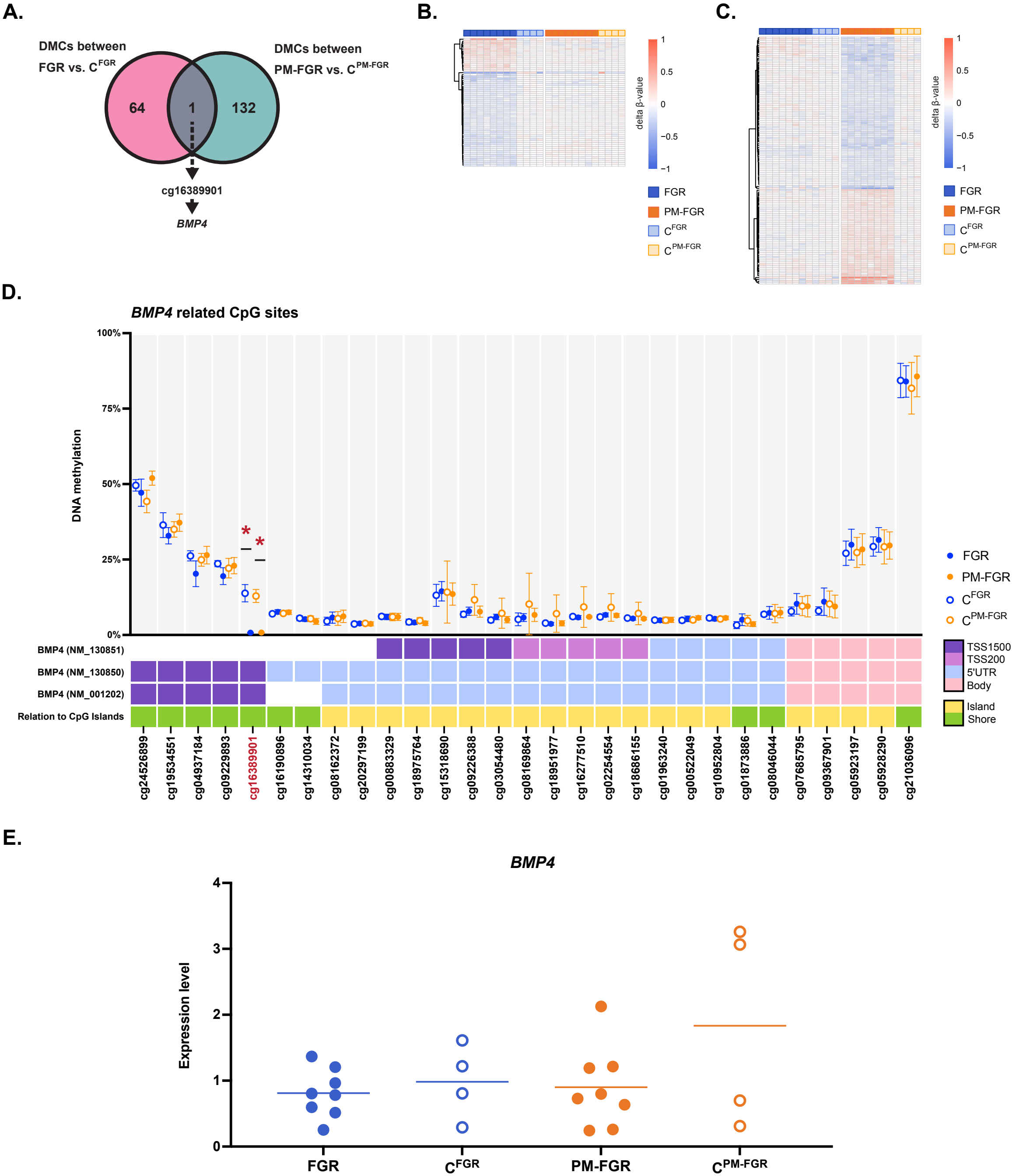
A.
DMCs between FGR vs. C^FGR
DMCs between PM-FGR vs. C^PM-FGR
64
1
132
cg16389901
BMP4
B.
delta β-value
1
0.5
0
−0.5
−1
FGR
PM-FGR
C^FGR
C^PM-FGR
C.
delta β-value
1
0.5
0
−0.5
−1
FGR
PM-FGR
C^FGR
C^PM-FGR
D.
BMP4 related CpG sites
DNA methylation
100%
75%
50%
25%
0%
*
*
FGR
PM-FGR
C^FGR
C^PM-FGR
BMP4 (NM_130851)
BMP4 (NM_130850)
BMP4 (NM_001202)
Relation to CpG Islands
TSS1500
TSS200
5'UTR
Body
Island
Shore
cg24526899
cg19534551
cg04937184
cg09229893
cg16389901
cg16190896
cg14310034
cg08162372
cg20297199
cg00883329
cg18975764
cg15318690
cg09226388
cg03054480
cg08169864
cg18951977
cg16277510
cg12254554
cg08686155
cg01963240
cg00522049
cg10952804
cg11873886
cg08046044
cg07685795
cg09367901
cg05923197
cg05928290
cg21036096
E.
BMP4
Expression level
4
3
2
1
0
FGR
C^FGR
PM-FGR
C^PM-FGR

Figure 4.

A.

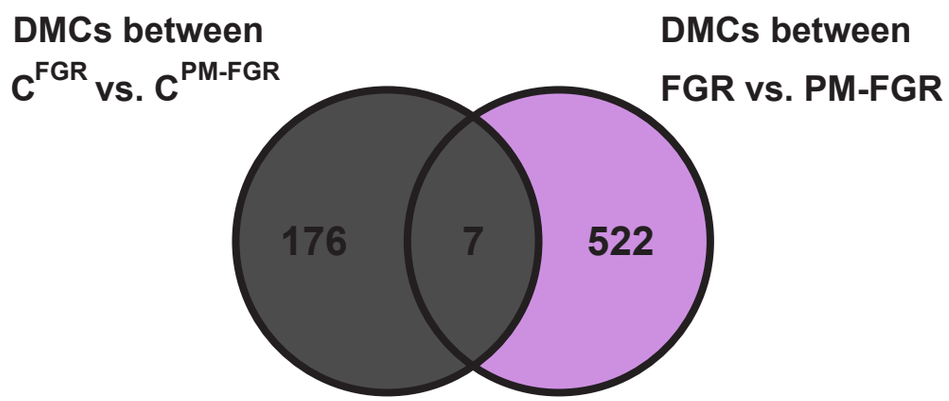

B.

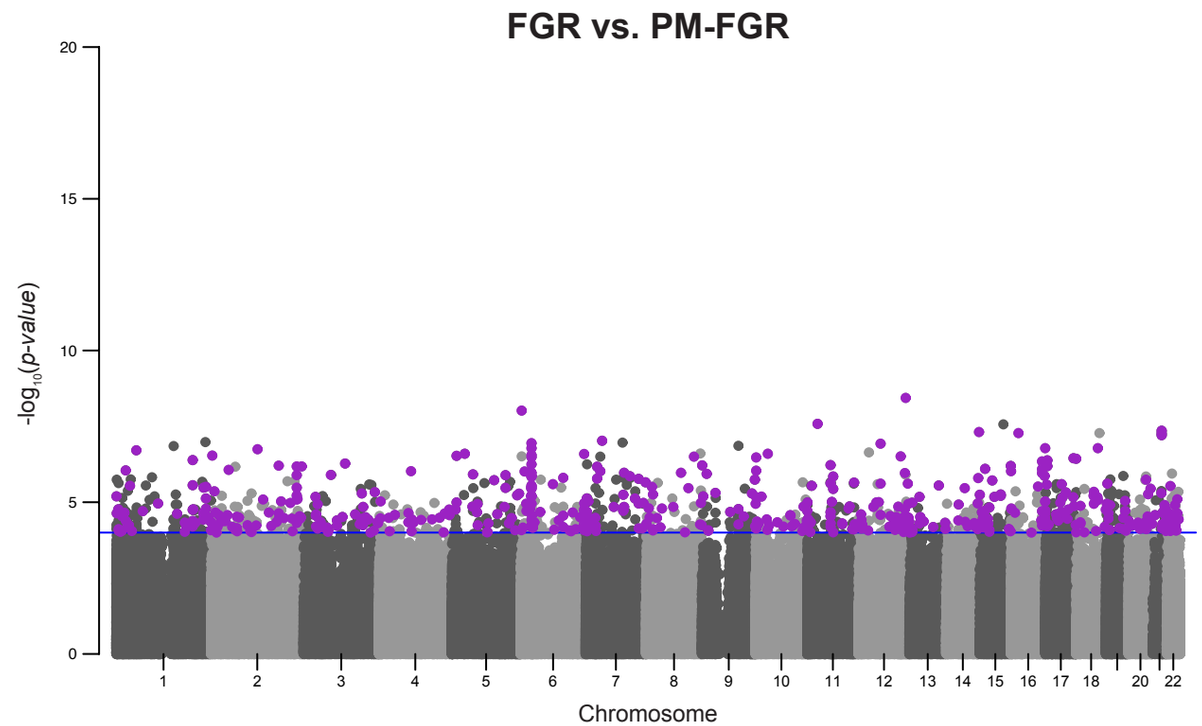

C.

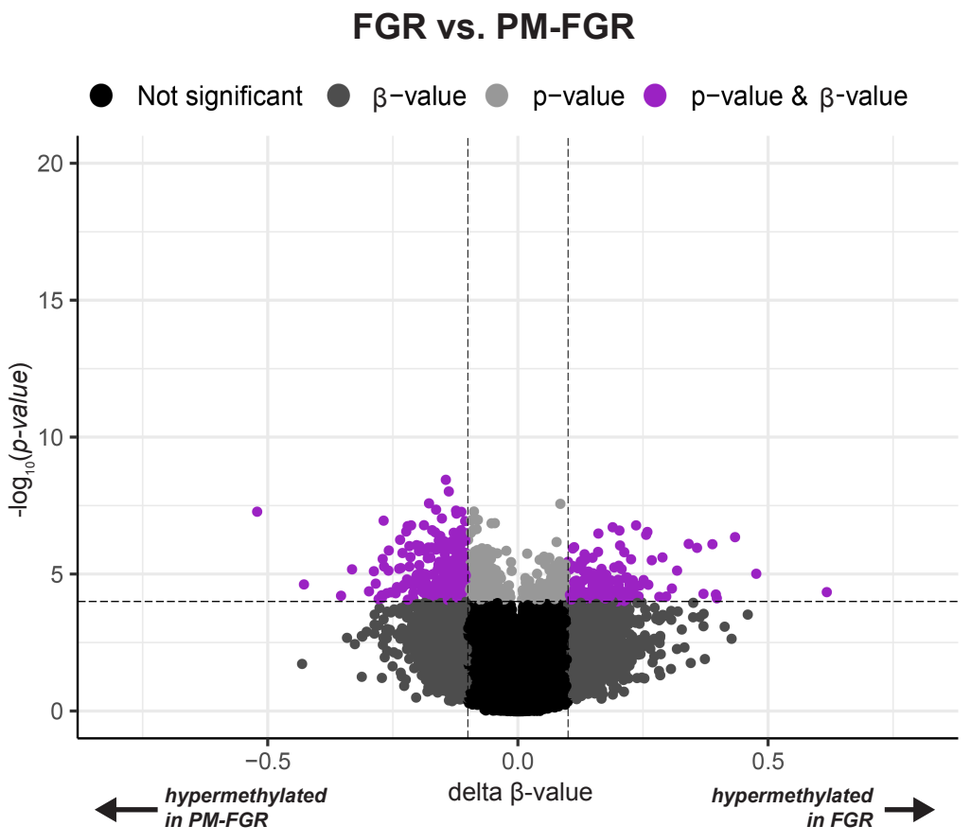

D.

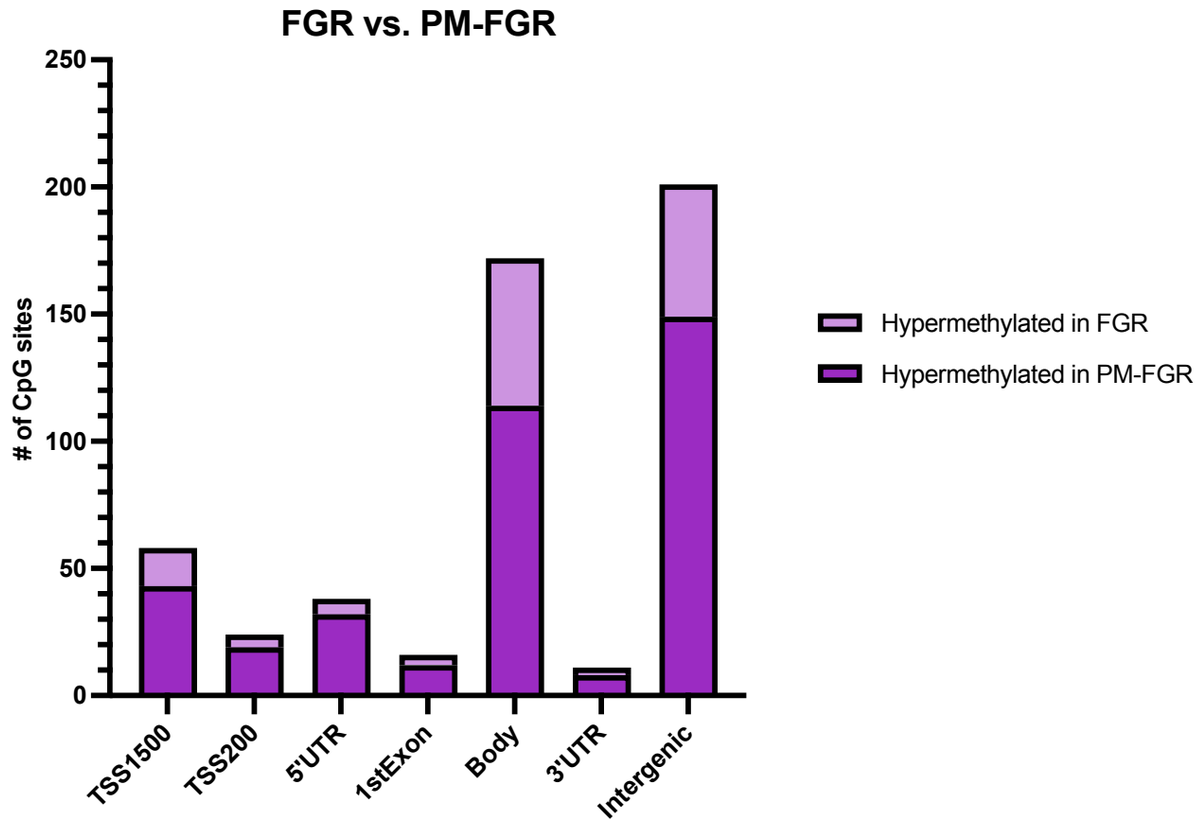

Figure 5.

A.

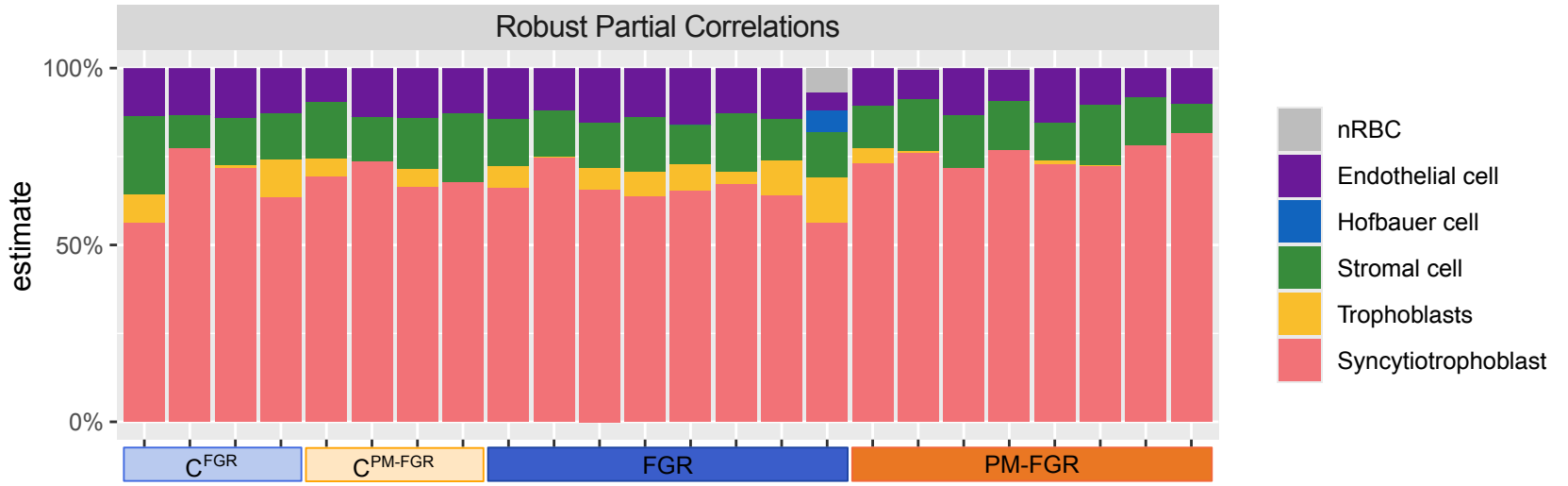

B.

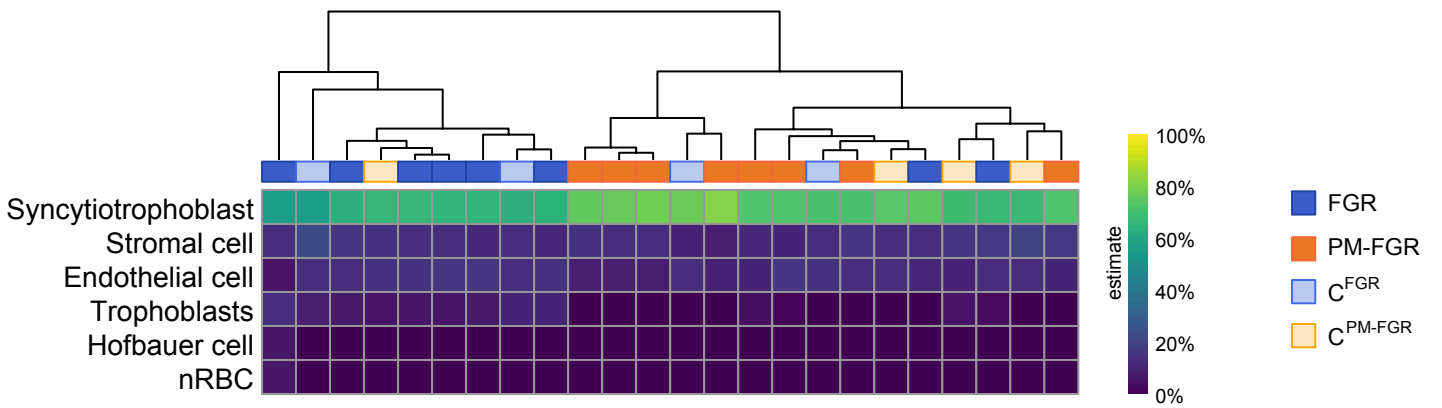

C.

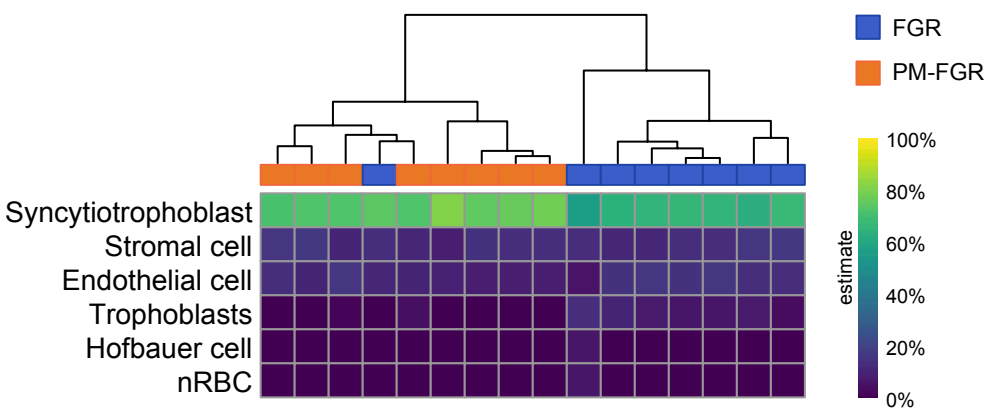
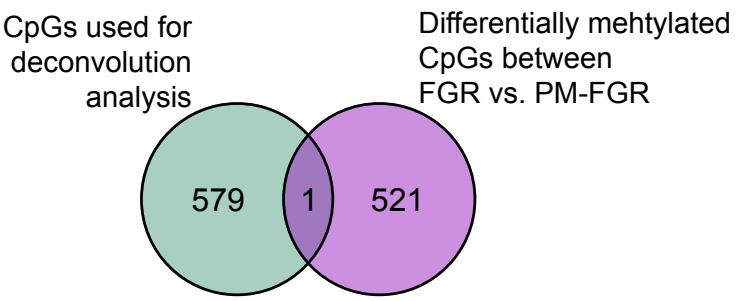
D.